OPEN

Agreement Between ^{18}F-FDG PET/CT and Whole-Body Magnetic Resonance Compared With Skeletal Survey for Initial Staging and Response at End-of-Treatment Evaluation of Patients With Multiple Myeloma

Nieves Gómez León, MD, PhD,† Beatriz Aguado Bueno, MD,‡ María Herreros Pérez, MD,†§ Luisa F. León Ramírez, MD,|| Adrián Alegre, MD, PhD,‡ Patrick M. Colletti, MD,¶ Domenico Rubello, MD, PhD,** José L. Carreras, MD, PhD,†† and Roberto C. Delgado Bolton, MD, PhD‡‡*

Purpose: To compare the agreement between whole-body (WB) magnetic resonance (MR) imaging, ^{18}F-FDG PET/CT, and skeletal survey (SS) in patients with multiple myeloma (MM) for diagnosis, initial staging, response evaluation, and early detection of complications.

Methods: This is a retrospective cohort study including MM patients who were diagnosed, treated, and followed in 2 institutions. These patients were studied with SS, WB-MR, and/or ^{18}F-FDG PET/CT. We studied bone lesions by anatomical locations and analyzed the concordance between SS and a tomographic technique (WB-MR or ^{18}F-FDG PET/CT) and between both tomographic techniques (WB-MR and PET/CT).

Results: Forty-four MM patients with a mean age of 62.6 years (range, 38–85 years) were included from January 2012 to February 2016. Whole-body MR and ^{18}F-FDG PET/CT found more lesions than SS in every location except in the skull. Concordance between WB-MR and ^{18}F-FDG PET/CT was either good or excellent in most of the locations and in plasmacytoma studies. However, WB-MR was better than ^{18}F-FDG PET/CT in the study of complications (medullar compression and vascular necrosis).

Conclusions: Our results suggest the study of MM patients should include WB-MR and/or ^{18}F-FDG PET/CT, whereas SS is only useful for the skull. Whole-body MR and ^{18}F-FDG PET/CT are complementary techniques, because both of them show good concordance in almost every location. It is still necessary to individualize the indication of each technique according to patient characteristics.

Key Words: ^{18}F-FDG PET/CT, MR, multiple myeloma, skeletal survey

(*Clin Nucl Med* 2021;46: 310–322)

Multiple myeloma (MM) is a hematological neoplasm based on a monoclonal proliferation of plasma cells.[1] It represents 10% of malignant hematologic neoplasms. This disease usually appears in the elderly, with a median age at diagnosis of 70 years and an incidence rate of 5.6/100,000 inhabitants per year. Its frequency is higher in males and African Americans.[2] The specific pathogenesis is unknown, but some environmental factors have been considered, such as herbicides, insecticides, benzene, or ionizing radiation.

In MM, a plasma cell clone has an uncontrolled proliferation in the bone marrow. Signs and symptoms of the disease are caused by the great amount of proteins and cytokines produced by these cells. Most MMs secrete immunoglobulin G (IgG) or IgA and light chains (kappa/lambda). It is denominated Bence-Jones MM when only light chains are produced (10% of cases). The MM neoplastic plasma cells also produce other proteins: cytokines. These factors are involved in some of the processes of the disease such as osteolysis or hypercalcemia. Occasionally, MMs are undetectable in serum or urine because they do not secrete proteins or cytokines.

Some of the most important clinical features of MM are those known by the acronym CRAB: calcium (elevated), renal failure, anemia, and bone lesions (osteopenia and lytic lesions). Clones of plasmatic cells can be found in the bone marrow (usually in axial and proximal appendicular skeleton) and soft tissues. Solitary plasmacytoma appears in fewer than 5% of patients with plasma cell neoplasms.

The diagnosis of MM is based on laboratory results (protein M, calcium, creatinine, and hemoglobin), cytological study (percentage of plasmatic cells in bone marrow aspiration), genetic studies (useful for prognosis), and imaging techniques (to evaluate bone lesions).

The definition of MM in 2003 was clinical-pathological, meaning the presence of symptoms caused by severe organ damage (osteolytic lesions or renal failure) was needed to reach a diagnosis, delaying the initiation of treatment. With the improvement in therapies, the available data showed that when patients initiated treatment earlier they had an increased survival. Because of this, the International Myeloma Working Group updated the diagnosis criteria for

Received for publication October 22, 2020; revision accepted December 3, 2020.
From the *University Hospital Research Institute, Department of Radiology, University Hospital La Princesa; †Autonomous University of Madrid; ‡Department of Haematology, University Hospital la Princesa of Madrid; §Department of Medicine, University Hospital Severo Ochoa, Leganés; ||Department of Nuclear Medicine, University Hospital Rey Juan Carlos, Móstoles, Madrid, Spain; ¶Department of Radiology, Keck School of Medicine of USC, Los Angeles, CA; **Department of Nuclear Medicine and PET Unit, Rovigo Hospital, Rovigo, Italy; ††Department of Nuclear Medicine, University Hospital Clínico San Carlos, Madrid; and ‡‡Department of Diagnostic Imaging (Radiology) and Nuclear Medicine, University Hospital San Pedro and Centre for Biomedical Research of La Rioja (CIBIR), Logroño, La Rioja, Spain.
All procedures performed in studies involving human participants were in accordance with the ethical standards of the institutional and/or national research committee and with the 1964 Helsinki Declaration and its later amendments or comparable ethical standards. An independent ethical committee for clinical research (Comité Ético de Investigación Clínica del Hospital Universitario de La Princesa de La Rioja, CEIC del HU La Princesa) approved the study design (Ref. CEIC-HLPR P.I. 892) in Spain in December 2015.
Conflicts of interest and sources of funding: none declared.
Correspondence to: Roberto C. Delgado Bolton, MD, PhD, Department of Diagnostic Imaging (Radiology) and Nuclear Medicine, University Hospital San Pedro and Centre for Biomedical Research of La Rioja (CIBIR), C/ Piqueras 98, Logroño 26006, La Rioja, Spain. E-mail: rbiolton@gmail.com.

ISSN: 0363-9762/21/4604–0310
DOI: 10.1097/RLU.0000000000003512

MM and smoldering MM.[3] In the update, 3 biomarkers were added as MM defining criteria, one of them based on the fact that new imaging techniques such as low-dose body CT, magnetic resonance (MR), and ^{18}F-FDG PET and PET/CT are more sensitive in detecting MM and must be considered in diagnosis and monitoring. The radiological biomarker is considered as having an MR with more than 1 focal lesion that must be at least 5 mm or more in size. The recommended follow-up examinations should be every 3 to 6 months in cases with a solitary focal lesion, equivocal findings, or diffuse infiltration.[3]

Current radiological techniques for the evaluation of bone damage in MM are skeletal survey (SS), whole-body (WB), and whole-spine MR and ^{18}F-FDG PET/CT.[4] Skeletal survey is still included in the initial evaluation of MM according to the 2009 International Myeloma Working Group recommendations.[5] However, the sensitivity of SS is not enough to detect early osteolytic lesions, and up to 30% of them cannot be observed with this technique.[6,7]

In 2013, a bibliographic review compared different techniques for the assessment of bone damage in MM including MR, ^{18}F-FDG PET, and SS. Magnetic resonance and ^{18}F-FDG PET showed higher sensitivity than SS and were able to detect bone lesions in 80% of patients.[8,9] Because there is no definitive agreement yet about the use of each of these new imaging techniques, it depends on the availability in each medical center. Up to now, few studies have been published comparing MR and ^{18}F-FDG PET in MM,[6,10,11] but there is evidence of the increased accuracy of ^{18}F-FDG PET/CT in many other tumor types.[12] Therefore, we propose a study that intends to bring new evidence and thus try to clarify which is the most adequate diagnostic approach. Whole-body MR and ^{18}F-FDG PET/CT detect larger extension of disease in MM than SS. There is no agreement yet about the use of these new imaging techniques. The aim of our study was to retrospectively compare WB-MR and ^{18}F-FDG PET/CT in the detection of bone involvement in the diagnosis and follow-up of patients with MM and the usefulness of each technique in different stages of the disease.

MATERIALS AND METHODS

Study Design and Patients

This is a retrospective cohort study including MM patients who were diagnosed, treated, and followed in 2 university hospitals. These patients were studied with SS, WB-MR, and/or ^{18}F-FDG PET/CT. At least 2 imaging techniques (SS, WB-MR, and/or ^{18}F-FDG PET/CT) were performed in these patients to evaluate MM bone lesions. These patients were followed from January 2012 until February 2016. We recruited patients from 2 departments of hematology of 2 university hospitals. Each hospital evaluated the criteria to diagnose and stage the MM, the extent of bone disease, and the clinical and radiological response to treatment.

Inclusion criteria were as follows: (*a*) patients with an initial diagnosis of MM, who had not been previously imaged with SS, WB-MR, or ^{18}F-FDG PET/CT and who had not received treatment for this diagnosis; (*b*) patients younger than 70 years old and candidates to bone marrow transplantation; (*c*) patients who had signed the informed consent following the instructions and rules of the ethics committee of each participating center for imaging techniques; (*d*) patients in whom the time delay between ^{18}F-FDG PET/CT and WB-MR was maximum 30 days. Exclusion criteria were as follows: (*a*) a life expectancy of less than 3 months, (*b*) a bad clinical condition, and (*c*) the rejection of the signed informed consent at any time during the study.

Finally, 44 patients who met these inclusion and exclusion criteria were included in the study. The flowchart for participant selection is presented in Figure 1.

Ethical Approval

All procedures performed in studies involving human participants were in accordance with the ethical standards of the institutional and/or national research committee and with the 1964 Helsinki Declaration and its later amendments or comparable ethical standards. An independent ethical committee for clinical research (Comité Ético de Investigación Clínica del Hospital Universitario de La Princesa, CEIC del H.U. de La Princesa) approved the study design (Ref. CEIC-HLPR P.I. 892) in Spain in December 2015.

Skeletal Survey

Conventional radiography is the imaging technique of choice in the initial diagnosis of MM and is still considered the criterion standard to determine the extent of the MM. It has great accuracy for detecting osteolytic lesions, especially those located in the skull. The SS procedure followed in our study included anteroposterior views of the thorax, cervical, dorsal, and lumbar spine; pelvis; and upper and lower extremities and lateral views of the skull, cervical, dorsal, and lumbar spine. The analysis of the SS images included the presence or absence of lesions in every single anatomic region in both the axial and the appendicular skeleton.

Reference or Criterion Standard

The current reference standard is the SS, although the new criteria recommend performing a diagnostic imaging test with higher resolution, such as MR or ^{18}F-FDG PET, depending on the availability of each center. In our patients, the presence of MM was confirmed by (*a*) bone marrow aspiration or biopsy and (*b*) biopsies of other extranodal locations if there was a suspicion of infiltration based on the laboratory or imaging tests.

^{18}F-FDG PET/CT

PET/CT studies were performed in the same PET/CT system with a 6-row detector CT (Biograph 6 TruePoint; Siemens Healthcare, Erlangen, Germany) with a theoretical spatial resolution of 3 to 4 mm. It is composed of 4 rows of detectors with LSO crystals and 6-row-detector CT with a system of dose modulation depending on the topogram (CARE Dose; Siemens Healthcare). The acquisition mode was 3-dimensional, with a coincidence detection window of 4.1 ns. The ^{18}F-FDG PET/CT procedure was identical for all the patients included, as described below.

Patient Preparation and ^{18}F-FDG PET/CT Study Protocol

In all patients, the European Association of Nuclear Medicine procedure guidelines for ^{18}F-FDG PET/CT for tumor imaging version 2.0 were followed.[13]

The day of the procedure, before administering ^{18}F-FDG, all patients underwent a short and directed clinical history in order to obtain the most relevant information (oncologic history, comorbidities such as inflammatory or infectious processes, diabetes mellitus), explanation of the procedure, and signing of the informed consent for administration of the intravenous contrast.

Patients were fasted for a minimum of 6 hours (except in patients with diabetes mellitus), and adequate hydration was recommended as 1 L in the 2 hours before ^{18}F-FDG administration). Patients were asked to avoid strenuous exercise during the 24 h before the procedure. Blood glucose was always verified before ^{18}F-FDG administration with an upper threshold of 200 mg/dL. ^{18}F-FDG dosage was 5 MBq per kg of weight using an automatic

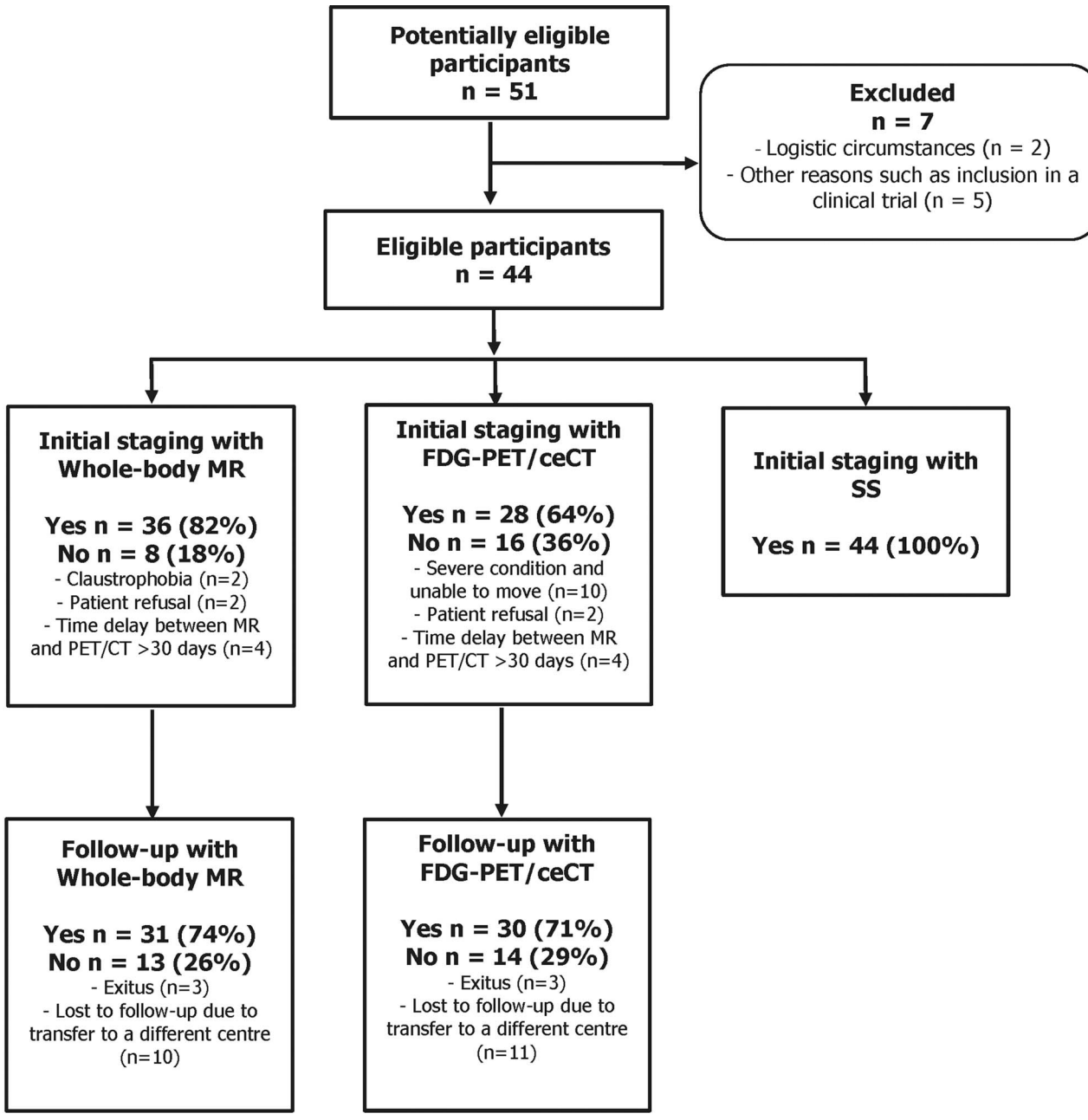

FIGURE 1. Flowchart of patient participation.

injector (Medrad Intego 200, Bayer HealthCare, MEDRAD Europe, the Netherlands). All patients had an uptake period of 45 to 60 minutes in a quiet room. The ^{18}F-FDG PET/CT procedure was performed following the European Association of Nuclear Medicine guidelines,[13] administering 130 mL of iodinated contrast (with a delay of 45 seconds and a speed of 2.5 mL/s) if not contraindicated. First, a thoracic CT in deep inspiration was performed to acquire images of the arterial phase (110 kV and 60 mAs, pitch of 1.2, and 2.5-mm thickness), followed by a WB CT in portal phase (110 kV and 95 mAs, 0.5-second tube rotation, pitch of 6, and a thickness of 5 mm) with a craniocaudal scan including from the top of the skull to the distal extremity of the thighs. The image was acquired with a 512 matrix and a 1-mm pixel. Then, PET was acquired from caudal to cranial with 3-minute beds and 20% overrun. Iterative reconstruction was applied. Regarding the coaxial range of the scan, WB imaging was performed, from the top of the head through the feet.[13]

^{18}F-FDG PET/CT Interpretation and Image Analysis

Studies were analyzed by a nuclear medicine physician and a radiologist in agreement, all with experience in the field using the same workstation (Syngo software system; Siemens Medical Imaging, Erlangen, Germany). Both readings were done independently with a consensus generated post hoc and discrepancies resolved by discussion. Independent reading of the CT component of the ^{18}F-FDG PET/CT was not considered in our study as reading ^{18}F-FDG PET/CT as a whole is a technique validated more than a decade ago.

Regarding the analysis of the ^{18}F-FDG PET/CT images related to the clinical suspicion in each patient, we took into account all the suspected regions that could present MM involvement based on the available data (clinical history, analysis, and imaging). These regions were analyzed in the ^{18}F-FDG PET/CT study to evaluate if they presented increased uptake of ^{18}F-FDG and, when they did, if they were suggestive of MM based on the metabolic information supplied by ^{18}F-FDG PET and the lytic lesions detected on the CT. We also made a semiquantitative analysis of the increased ^{18}F-FDG uptakes comparing them with other areas of physiological uptake. The criteria applied for reading the images and classifying the findings as positive or negative were :

(1) Visual analysis: the results of the ^{18}F-FDG PET/CT were considered positive or negative for MM lesions classifying the results in 4 categories: (*a*) the presence of a pathological ^{18}F-FDG uptake was considered an active MM lesion when there was an increased and suspicious ^{18}F-FDG uptake in the region where there was a lytic lesion suggestive of MM, independently of the intensity, distribution, and extent of the ^{18}F-FDG uptake, categorizing the ^{18}F-FDG PET/CT study as positive for an active MM lesion in that location; (*b*) the presence of a pathological FDG uptake was considered an active MM lesion when there was an increased and suspicious ^{18}F-FDG uptake even if there were no underlying lytic lesions, independently of the intensity, distribution, and extent of the ^{18}F-FDG uptake, categorizing the ^{18}F-FDG PET/CT study as positive for an incipient active MM; (*c*) the absence of an increased and suspicious ^{18}F-FDG uptake in the region where there was a lytic lesion suggestive of MM, categorizing the ^{18}F-FDG PET/CT study as an inactive MM lesion in that location; and (*d*) the absence of an increased and suspicious ^{18}F-FDG uptake and no detectable lytic lesions suggestive of MM, categorizing the ^{18}F-FDG PET/CT study as negative for MM.
(2) Semiquantitative analysis: SUVmax was measured in the increased ^{18}F-FDG uptake and was compared with the physiological uptake (measured as SUVmax) in 2 regions: (*a*) the mediastinal blood pool (MBP), calculated measuring a volume of interest (VOI) with a diameter of 3 mm inside the walls of the ascending aorta; and (*b*) the liver uptake, calculated measuring VOI with a diameter of 3 cm drawn in the right hepatic lobe trying to exclude from the VOI any areas of inhomogeneous or focally increased uptake (physiological, pathological, or due to artifacts). A five-point scale was applied using these references: 0 was considered for the absence of pathological uptake; 1 when the uptake (SUVmax) was lower than the MBP; 2 when the uptake (SUVmax) was higher than the MBP but lower than the liver; 3 when the uptake (SUVmax) was higher than the liver without duplicating the SUVmax; 4 when the uptake (SUVmax) was more than double than the liver uptake.

MR Study Protocol, Interpretation, and Image Analysis

A WB and whole-spine MR (WB-MR) study was performed following standard protocols including contrast enhancement in certain cases. A GE 1.5-T magnet (GE Healthcare, Milwaukee, WI) was used. The sequences used include (*a*) coronal T1-weighted (turbo spin-echo) and short tau (or TI) inversion recovery (STIR) sequences from head to ankles; (*b*) sagittal T1-weighted and STIR sequences of the entire spine with postprocessing imaging pasting in both cases; and (*c*) diffusion-weighted imaging sequences, including diffusion-weighted WB imaging with background body signal suppression and analysis of diffusion restriction. Intravenous contrast was administered in patients with normal renal function and unsuspected diagnosis of MM. Regarding the coaxial range of the scan, WB imaging was performed, from the top of the head to the ankles. The scanning protocol includes, first, chest and abdomen scanning with T1-weighted (turbo spin-echo) and STIR sequences; and second, sagittal scanning ranges to cover the entire spine in the same T1-weighted and STIR sequences.

The interpretation of the WB-MR images is the same as the one used in SS for every anatomic region. Lesions detected by MR were defined by an alteration of signal intensity and their morphology in T1, STIR, and diffusion-weighted WB imaging with background body signal suppression sequences.

Skeletal Survey Protocol, Interpretation, and Image Analysis

Conventional radiography is the imaging technique of choice in the initial diagnosis of MM and is still considered the criterion standard to determine the extent of the MM. It has great accuracy for detecting osteolytic lesions, especially those located in skull. The SS procedure followed in our study (in both centers) included anteroposterior views of the thorax, cervical, dorsal, and lumbar spine; pelvis; and upper and lower extremities and lateral views of the skull, cervical, dorsal, and lumbar spine. The analysis of the SS images included the presence or absence of lesions in every single anatomic region in both the axial and the appendicular skeleton.

Statistical Analysis

For the descriptive analysis, the qualitative variables analyzed were presented with their distribution of frequency and percentages, whereas the quantitative variables analyzed were presented with the mean and SD. An analysis of the validity was performed. Agreement between each diagnostic technique with the criterion standard was also calculated (κ coefficient and 95% confidence intervals. All statistical tests were considered bilateral, and significant results were considered when a statistical significance of $P < 0.05$ was achieved.

The statistical program used was IBM SPSS version 24.0.

RESULTS

Between January 2012 and February 2016, 44 MM patients were included. At least 2 imaging techniques (SS, WB-MR, and/or ^{18}F-FDG PET/CT) were performed in these patients to evaluate MM bone lesions. The 44 MM patients (24 women and 20 men) had a mean age of 62.6 years ±11.4 (range, 38–85 years). All of them were diagnosed with MM of the following types: 47.6% were IgG; 16.7%, IgA; 14.3%, nonsecretory; and 19.1%, other types. The flowchart for participant selection is presented in Figure 1. The clinical variables collected were the extent of bone disease and the response to treatment after induction therapy, following autologous transplantation, and during follow-up. Table 1 presents the characteristics of the patients at baseline.

Radiological Studies. Lesion Analysis

The data of the 3 imaging techniques (SS, WB-MR, and ^{18}F-FDG PET/CT) were grouped and analyzed by (*a*) anatomic regions, considering more than 10 different regions, and (*b*) axial/appendicular regions, considering 2 groups: the spinal column (that included the cervical, dorsal, and lumbar column) and the appendicular skeleton (that included the pelvis, upper extremities, lower extremities, and clavicles). The regions studied included

TABLE 1. Characteristics of the Patients at Baseline

Characteristics of the Patients at Baseline (n = 44)			
Parameter		**Frequency**	**Percentage**
Sex	Female	24	54.5
	Male	20	45.5
MM subtype	IgA	7	15.9
	IgG	20	45.5
	IgA + IgG	1	2.3
	Bence-Jones	6	13.6
	Nonsecretor	6	13.6
	Plasmacytoma	3	6.8
	Lost to follow-up	1	2.3
Light chain	Kappa	21	47.7
	Lambda	18	40.9
	Lost to follow-up	5	11.4
Clinical stage	IA	2	4.5
	IB	0	0
	IIA	11	25.0
	IIB	0	0
	IIIA	17	38.6
	IIIB	5	11.4
	Lost to follow-up	9	20.5
Induction chemotherapy	No treatment	4	9.1
	VBMCT/VBAD	5	11.4
	VAD	2	4.5
	PAD	5	11.4
	VISTA (M + P + B)	2	4.5
	MP	1	2.3
	DV (BD)	11	2.0
	MP + VAD	4	9.1
	VRD	4	9.1
	TD	3	6.8
	Lost to follow-up	3	6.8
Radiotherapy	Yes	14	31.8
	No	30	68.2
Transplantation	Yes	24	54.5
	No	20	45.5
Plasmacytoma	Yes	14	31.8
	No	30	68.2
Initial SS	Yes (SS done)	44	100.0
	No/no access	0	0
Initial WB-MR	Yes (MR done)	36	81.8
	No	8	18.2
Initial ^{18}F-FDG PET/CT	Yes (PET done)	28	63.6
	No	16	36.4
Follow-up WB-MR	Yes (MR done)	31	70.5
	No	13	29.5
Follow-up ^{18}F-FDG PET/CT	Yes (PET done)	30	68.2
	No	14	31.8
Patients in which lesions were detected or not with SS	Yes (patients in which lesions were detected with SS)	21	47.7
	No	23	52.3

VBMCT/VBAD, vincristine, carmustine, melphalan, cyclophosphamide and prednisone alternating with vincristine, carmustine, doxorubicin, and dexamethasone; VAD, vincristine, adriamycin, dexamethasone; PAD, bortezomib (Velcade), adriamycin, dexamethasone; VISTA, bortezomib (Velcade), melphalan, prednisone; MP, melphalan, prednisone; BD, bortezomib (Velcade), dexamethasone; VRD, bortezomib (Velcade), lenalidomide, dexamethasone.

the skull, sternum, and ribs independently because of their special anatomic features as flat bones. For WB-MR and ^{18}F-FDG PET/CT, the evaluation included MM complications and the presence of plasmacytoma and complications.

In the SS, 21 patients had lesions detected in at least 1 location, and in 23 patients, the study was negative in all locations (Table 1). On the other hand, in WB-MR and ^{18}F-FDG PET/CT, lesions were found in all studies at diagnosis in at least 1 location. Table 2 presents the results of the SS, whereas the following 2 tables present the agreement or concordance between SS and WB-MR (Table 3) and between SS and ^{18}F-FDG PET/CT (Table 4). The skull showed lytic lesions in 16 cases in SS (Table 2); one of these cases was not detected with WB-MR (Table 3), and 4 of them were not detected with ^{18}F-FDG PET/CT (Table 4). In this regard, the lower detection rate of the CT component of the ^{18}F-FDG PET/CT compared with SS in the evaluation of skull lesions could be due to interpretation issues related to false-negative reading of the ^{18}F-FDG PET/CT.

^{18}F-FDG PET/CT for Initial Staging and Response Monitoring at the End of Treatment

Of the 16 patients without ^{18}F-FDG PET/CT examinations at diagnosis, 10 of them were unable to undergo these procedures because of their severe clinical condition. The other 6 studies were not performed because patients refused to undergo the examination (n = 2) or because more than 30 days had passed between ^{18}F-FDG PET/CT and the other imaging techniques (n = 4).

Follow-up with ^{18}F-FDG PET/CT was performed in 30 patients. In the remaining 14 patients, follow-up with ^{18}F-FDG PET/CT was not done because of exitus (n = 3), that is, patient death, or because they were lost during follow-up because of a transfer to another center (n = 11).

Table 4 presents the agreement or concordance between SS and ^{18}F-FDG PET/CT.

WB-MR for Initial Staging and Response Monitoring at the End of Treatment

Eight WB-MR studies at diagnosis were not registered. The reasons were the patient's intolerance to the technique (2 were claustrophobic patients, and 2 other patients refused to undergo

TABLE 2. Results of the SS in All Patients

Results of the Skeletal Survey (SS) in All Patients (n = 44)			
Region		**SS (+)**	**SS (−)**
Skull		21	23
Spine vertebrae	Any location	6	38
	Cervical	1	43
	Dorsal	4	40
	Lumbar	4	40
Sternum		0	44
Ribs		8	36
Appendicular skeleton	Pelvis	9	35
	Superior limbs	11*	33
	Inferior limbs	7	37
	Clavicles	8	36

*In the upper limbs, SS detected lesions in 11 patients, but only in 5 of these patients the lesions found with SS could be compared with WB-MR and ^{18}F-FDG PET/CT because these tomographic techniques do not always include the upper limbs.

TABLE 3. Agreement or Concordance Between SS and WB-MR, Quantified Regarding the Patients Who Have Had at Least 1 Lesion Detected With the Test (SS or WB-MR) in Each of the Regions Described

Agreement Between WB-MR Versus SS for Patients (n) Who Have Had at Least 1 Lesion Detected With the Test (SS or WB-MR) in the Regions Described

Regions		Concordance Coincidences		SS (−) WB-MR (+)	SS (+) WB-MR (−)	κ	*P*
		Positive (+)	Negative (−)				
Skull*		11	13	0	2*	0.846	0.001
Spine vertebrae	Any location	5	12	19	0	0.149	0.088
	Cervical†	0	20	13	0	—†	—†
	Dorsal	3	14	19	0	0.064	0.149
	Lumbar	3	16	18	0	0.126	0.115
Sternum‡		0	18	13	0	—‡	—‡
Ribs		8	12	11	0	0.360	0.009
Appendicular skeleton§	Any location	13	1	18	0	0.043	0.401
	Pelvis	7	13	15	0	0.257	0.023
	Superior limbs‖	3	16	8	0‖	0.308	0.027
	Inferior limbs	5	11	11	0	0.270	0.040
	Clavicles	4	18	8	0	0.375	0.009

*Discordances in the skull: SS (+) and WB-MR (−).

†No statistics have been calculated because SS in the cervical spine is a constant (no lesion).

‡No statistics have been calculated because SS in the sternum is a constant (no lesion).

§No statistics have been calculated because WB-MR in the appendicular skeleton is a constant (all the positive cases).

‖Superior limbs: in the upper limbs, SS detected lesions in 11 patients, but only in 5 of these patients the lesions found with SS could be compared with WB-MR and FDG PET/CT because these tomographic techniques do not always include the upper limbs. On the other hand, WB-MR detected lesions in 11 patients, 3 of them compared and confirmed on SS (SS and WB-MR concordant in 3), but in the other 8 patients, the lesions detected with WB-MR were not detectable on SS (SS negative and WB-MR positive in 8).

TABLE 4. Agreement or Concordance Between SS and ^{18}F-FDG PET/CT, Quantified Regarding the Patients Who Have Had at Least 1 Lesion Detected With the Test (SS or ^{18}F-FDG PET/CT) in Each of the Regions Described

Agreement Between ^{18}F-FDG PET/CT Versus SS for Patients (n) Who Have Had at Least 1 Lesion Detected With the Test (SS or ^{18}F-FDG PET/CT) in the Regions Described

Regions		Concordance Coincidences		SS (−) PET/CT (+)	SS (+) PET/CT (−)	κ	*P*
		Positive (+)	Negative (−)				
Skull*		10	11	0	6*	0.590	0.001
Spine vertebrae	Any location	5	11	12	0	0.247	0.047
	Cervical†	0	21	7	0	—†	—†
	Dorsal	3	12	13	0	0.165	0.112
	Lumbar	3	15	10	0	0.243	0.049
Sternum‡		0	16	12	0	—‡	—‡
Ribs		6	9	13	0	0.229	0.057
Appendicular skeleton§	Any location	10	3	14	0	0.071	0.527
	Pelvis	6	12	10	0	0.340	0.017
	Superior limbs‖	4	13	9	0‖	0.308	0.030
	Inferior limbs	3	16	9	0	0.276	0.034
	Clavicles	2	18	8	0	0.243	0.049

*Discordances in the skull: SS (+) and WB-MR (−).

†No statistics have been calculated because SS in the cervical spine is a constant (no lesion).

‡No statistics have been calculated because SS in the sternum is a constant (no lesion).

§No statistics have been calculated because WB-MR in the appendicular skeleton is a constant (all the positive cases).

‖Superior limbs: in the upper limbs, SS detected lesions in 11 patients, but only in 5 of these patients the lesions found with SS could be compared with WB-MR and ^{18}F-FDG PET/CT because these tomographic techniques do not always include the upper limbs. Regarding ^{18}F-FDG PET/CT, it detected lesions in 13 patients, 4 of them compared and confirmed on SS (SS and ^{18}F-FDG PET/CT concordant in 4), but in the other 9 patients, the lesions detected with ^{18}F-FDG PET/CT were not detectable on SS (SS negative and ^{18}F-FDG PET/CT positive in 9).

the procedure) or because more than 30 days had passed between WB-MR and the other imaging studies (n = 4).

Regarding the follow-up with WB-MR, it was done in 31 patients. In the remaining 13 patients, follow-up with WB-MR was not done because of exitus (n = 3), that is, patient death, or because they were lost during follow-up because of a transfer to another center (n = 10).

Table 3 presents the agreement or concordance between SS and WB-MR for initial staging.

Region Analysis With All the Tests: Description of the Results

The skull is the only region where SS is superior to ^{18}F-FDG PET/CT and WB-MR. Skeletal survey visualizes lytic lesions in any location. All patients with lytic lesions in the skull (n = 21) were detected by SS. Whereas SS detected lesions in the skull in 21 patients, MR detected 11 positive cases, and ^{18}F-FDG PET/CT detected 10 positive cases.

Tomographic techniques (WB-MR and ^{18}F-FDG PET/CT) were superior to SS in the rest of the locations. In the cervical spine, the SS detected only 1 case (Table 2), whereas WB-MR detected bone lesions in 13 other cases (SS negative and WB-MR positive), and ^{18}F-FDG PET/CT in 7 other cases (SS negative and ^{18}F-FDG PET/CT positive). In the dorsal spine, SS detected 4 cases, whereas WB-MR and ^{18}F-FDG PET/CT detected 22 cases (SS and WB-MR concordant in 3, SS negative and WB-MR positive in 19) and 16 cases (SS and ^{18}F-FDG PET/CT concordant in 3, SS negative and ^{18}F-FDG PET/CT positive in 13), respectively. In the lumbar spine, SS detected 4 cases, whereas WB-MR and ^{18}F-FDG PET/CT detected 21 cases (SS and WB-MR concordant in 3, SS negative and WB-MR positive in 18) and 13 cases (SS and ^{18}F-FDG PET/CT concordant in 3, SS negative and ^{18}F-FDG PET/CT positive in 10), respectively. The sternum was considered in this study as an isolated location because it is a flat bone. Skeletal survey was negative in this location in all patients. All lesions at this location were positive in WB-MR in 13 patients (SS negative and WB-MR positive) and positive in ^{18}F-FDG PET/CT in 12 patients (SS negative and ^{18}F-FDG PET/CT positive). The rib cage was also considered in this study as an isolated location. Skeletal survey was positive in 8 cases, compared with 19 detected both by WB-MR (SS and WB-MR concordant in 8, SS negative and WB-MR positive in 11) and ^{18}F-FDG PET/CT (SS and ^{18}F-FDG PET/CT concordant in 6, SS negative and ^{18}F-FDG PET/CT positive in 13). In all cases where SS was positive, WB-MR and/or ^{18}F-FDG PET/CT were also positive.

Comparison of the Initial Staging With Both Tests ^{18}F-FDG PET/CT and WB-MR

The agreement between ^{18}F-FDG PET/CT and WB-MR was analyzed. Both studies in the pair had been performed at the same time point. Table 5 presents the agreement between initial WB-MR and ^{18}F-FDG PET/CT for lesions detected.

We observed very good agreement between WB-MR and ^{18}F-FDG PET/CT in lesions in the dorsal and lumbar column (κ = 0.831 and 0.779, respectively; $P < 0.0001$). We found lower agreement in the cervical column in WB-MR versus ^{18}F-FDG PET/CT (κ = 0.615; $P < 0.001$), whereas SS presented a very low detection rate in these locations (cervical, dorsal, and lumbar vertebrae). The study of sternum and ribs presented a good agreement between WB-MR and ^{18}F-FDG PET/CT with κ = 0.65 and 0.72, respectively ($P < 0.0001$ for both). On the other hand, SS could not find any lesions in the sternum, which is a great limitation to this technique. When assessing the ribs, only the largest lytic lesions were detected with SS, which is a great limitation to this technique, whereas WB-MR and ^{18}F-FDG PET/CT performed much better.

TABLE 5. Agreement or Concordance Between Pretreatment WB-MR and ^{18}F-FDG PET/CT, Quantified Regarding the Patients Who Have Had at Least 1 Lesion Detected With the Test (^{18}F-FDG PET/CT or WB-MR) in Each of the Regions Described

Agreement Between Pretreatment WB-MR Versus ^{18}F-FDG PET/CT for Patients (n) Who Have Had at Least 1 Lesion Detected With the Test (WB-MR or ^{18}F-FDG PET/CT) in the Regions Described

Regions		Concordance Coincidences		MR (+) PET/CT (−)	MR (−) PET/CT (+)	κ	*P*
		Positive (+)	Negative (−)				
Skull		6	8	4	1	0.481	0.027
Spine vertebrae	Any location	17	7	2	0	0.821	0.0001
	Cervical	8	13	5	0	0.615	0.001
	Dorsal	16	8	2	0	0.831	0.0001
	Lumbar	13	11	3	0	0.779	0.0001
Sternum		8	12	2	2	0.657	0.001
Ribs		14	7	2	1	0.727	0.0001
Appendicular skeleton	Any location	19	1	3	0	0.355	0.026
	Pelvis	14	8	1	2	0.746	0.0001
	Superior limbs	5	11	1	1	0.750	0.001
	Inferior limbs	10	9	1	0	0.900	0.0001
	Clavicle	8	12	2	1	0.732	0.0001
Plasmacytoma		8	10	0	0	1	0.0001
Lymph node infiltration		1	21	0	2	0.467	0.007
Avascular necrosis		0	17	0	2	—*	—*
Lymph node infiltration		2	21	3	0	0.519	0.003
Fractures		7	13	0	0	1	0.0001

*No statistics have been calculated because the avascular necrosis is a constant in ^{18}F-FDG PET/CT.

Comparison of Skeletal Survey With FDG PET/CT and WB-MR

In the pelvis, SS detected lesions in 9 patients, WB-MR in 22 (SS and WB-MR concordant in 7, SS negative and WB-MR positive in 15) and ^{18}F-FDG PET/CT in 16 (SS and ^{18}F-FDG PET/CT concordant in 6, SS negative and ^{18}F-FDG PET/CT positive in 10).

In the upper limbs, SS detected lesions in 11 patients (Table 2), but only in 5 of these patients the lesions found with SS could be compared with WB-MR and ^{18}F-FDG PET/CT because these tomographic techniques do not always include the upper limbs. On the other hand, WB-MR detected lesions in 11 patients, 3 of them compared and confirmed on SS (SS and WB-MR concordant in 3), but in the other 8 patients, the lesions detected with WB-MR were not detectable on SS (SS negative and WB-MR positive in 8). Regarding ^{18}F-FDG PET/CT, it detected lesions in 13 patients, 4 of them compared and confirmed on SS (SS and ^{18}F-FDG PET/CT concordant in 4), but in the other 9 patients, the lesions detected with FDG PET/CT were not detectable on SS (SS negative and ^{18}F-FDG PET/CT positive in 9).

Regarding the lower extremities, SS detected lesions in only 7 patients. Whole-body MR was positive in 16 patients. Skeletal survey and WB-MR were concordant in 5 cases (2 of the patients with SS did not have a WB-MR study), SS negative and WB-MR positive in 11. ^{18}F-FDG PET/CT detected lesions in 12 cases (SS and ^{18}F-FDG PET/CT concordant in 3 cases [4 out of seven positive cases in SS did not have PET/CT], SS negative and ^{18}F-FDG PET/CT positive in 9). In no case lesions were seen in SS that were not seen in WB-MR nor ^{18}F-FDG PET/CT. Figure 2 and Figure 3 show the case of a patient with MM presenting with multiple expansive lesions.

In the clavicles, 8 patients had lesions on SS. Whole-body MR was positive in 12 patients (SS and WB-MR concordant in 4, SS negative and WB-MR positive in 8). ^{18}F-FDG PET/CT detected lesions in 10 cases (SS and ^{18}F-FDG PET/CT concordant in 2, SS negative and ^{18}F-FDG PET/CT positive in 8).

Table 5 presents the agreement between pretreatment WB-MR and ^{18}F-FDG PET/CT, and Table 6 presents the agreement between posttreatment WB-MR and ^{18}F-FDG PET/CT.

Agreement or Concordance Analysis

The concordance analyses between SS and WB-MR, SS and ^{18}F-FDG PET/CT, and WB-MR and ^{18}F-FDG PET/CT are presented in Table 3, Table 4, and Table 5.

In the study of the bony pelvis, the concordance between WB-MR and ^{18}F-FDG PET/CT was good ($\kappa = 0.74$; $P < 0.0001$), whereas the SS does not visualize them.

In the upper and lower limbs, the concordance between WB-MR and ^{18}F-FDG PET/CT was excellent ($\kappa = 0.75$ and 0.90 respectively; $P < 0.0001$) and good in clavicles ($\kappa = 0.73$, $P < 0.0001$), whereas in the same regions, the study of concordance of both techniques with the SS was practically null.

With regard to the evaluation of plasmacytomas, in our study we found a good correlation between WB-MR and ^{18}F-FDG PET/CT ($\kappa = 0.84$; $P < 0.0001$). Figure 4 presents a case with a plasmacytoma in which there was concordance between all the techniques.

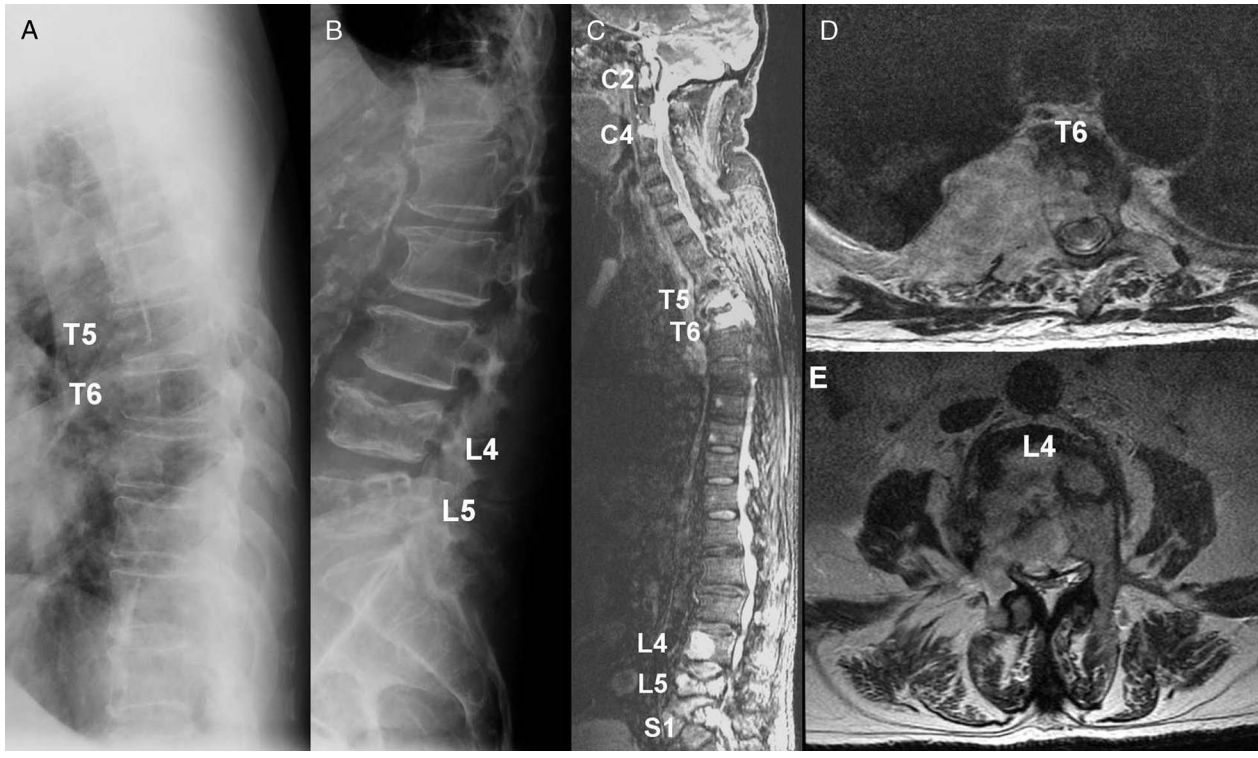

FIGURE 2. This 77-year-old man with diagnosis of MM presented with multiple expansive lesions in the right ribs. Dorsal (**A**) and lumbar (**B**) spine radiographies did not describe bone lesions on initial review. In retrospect, T5 and T6 may be more lucent than the adjacent vertebra. L4 and L5 compressions were initially interpreted as likely osteoporotic compression fractures. Whole column MR showed multiple bone lesions in cervical, thoracic, and lumbar levels (**C**). Thoracic axial STIR images (**D**) showed T6 tumor with posterior element invasion and impending cord compression. Lumbar axial STIR images (**E**) showed a prevertebral soft tissue mass and compression of the vertebral canal and nerve roots.

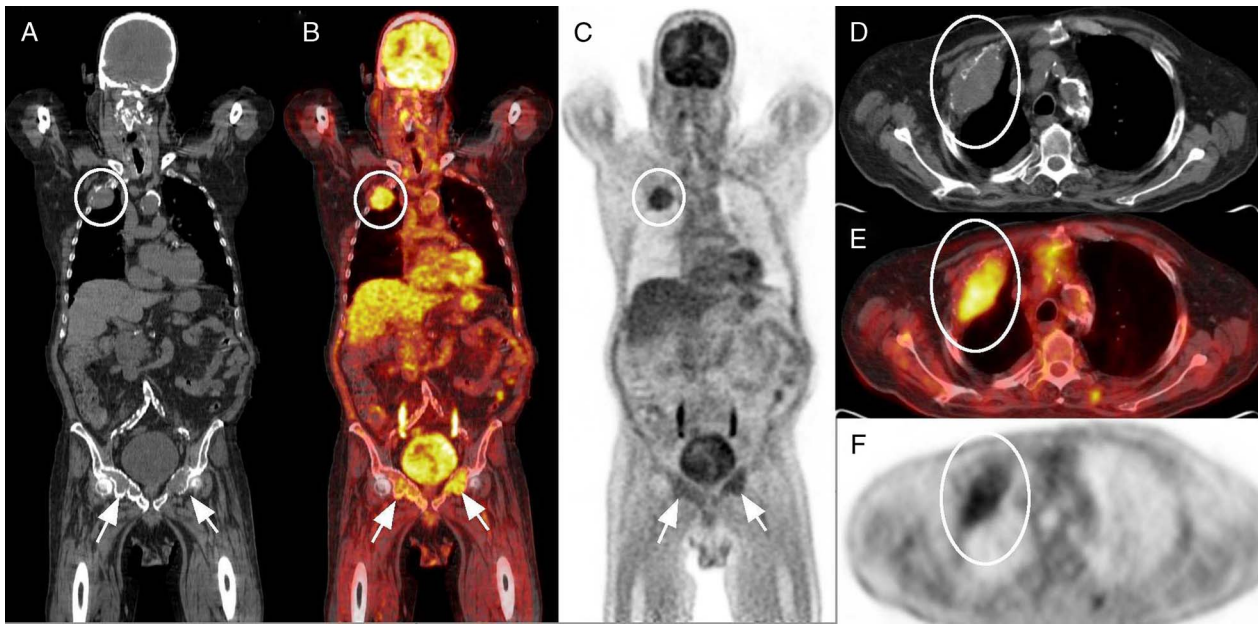

FIGURE 3. Additional images for the 77-year-old man with MM and multiple expansive lesions in the right ribs shown in Figure 2 are presented here. ^{18}F-FDG PET/CT demonstrated a destructive lesion with soft tissue mass in the right second rib with increased ^{18}F-FDG metabolism (SUVmax 4.5), as shown in the coronal and axial CT (**A**, **D**), fused ^{18}F-FDG PET/CT (**B**, **E**), and ^{18}F-FDG PET (**C**, **F**), respectively. The patient died after 3 cycles of chemotherapy due to treatment complications.

Additionally, we have analyzed lymph node involvement of MM. We found 6 of our MM patients presented with lymphatic involvement, all correctly detected with ^{18}F-FDG PET/CT but only 1 detected with WB-MR. Figure 5 presents one of these cases.

Finally, regarding complications, we have found 11 patients with spinal cord or medullary compression and 5 cases with avascular necrosis. In both complications, the WB-MR was superior to ^{18}F-FDG PET/CT, demonstrating improved detection. Figure 6

TABLE 6. Agreement or Concordance Between Posttreatment WB-MR and ^{18}F-FDG PET/CT, Quantified Regarding the Patients Who Have Had at Least 1 Lesion Detected With the Test (WB-MR or ^{18}F-FDG PET/CT) in Each of the Regions Described Regarding the Lesions Detected

Agreement Between Posttreatment WB-MR and Posttreatment ^{18}F-FDG PET/CT for Patients (n) Who Have Had at Least 1 Lesion Detected With the Test (WB-MR or ^{18}F-FDG PET/CT) in the Regions Described

Regions		Coincidences		MR (+) PET/CT (−)	MR (−) PET/CT (+)	κ	*P*
		Positive (+)	Negative (−)				
Skull		4	20	0	0	1	0.0001
Spine vertebrae	Any location	9	17	1	2	0.776	0.0001
	Cervical	2	19	5	1	0.289	0.088
	Dorsal	9	17	3	0	0.779	0.0001
	Lumbar	6	19	4	0	0.663	0.0001
Sternum		5	19	4	0	0.629	0.0001
Ribs		5	19	1	3	0.622	0.001
Appendicular skeleton	Any location	11	9	7	0	0.512	0.002
	Pelvis	7	12	7	3	0.303	0.089
	Superior limbs	3	19	0	0	1	0.0001
	Inferior limbs	1	21	1	1	0.455	0.026
	Clavicle	4	22	0	1	0.867	0.0001
Plasmacytoma		4	22	2	1	0.664	0.0001
Lymphadenopathic infiltration		0	26	0	3	—*	—*
Avascular necrosis		0	26	3	0	—†	—†
Medullary compression		1	22	6	0	0.202	0.071
Fractures		5	22	0	2	0.791	0.0001

*No statistics have been calculated because WB-MR lymph node involvement is a constant.

†No statistics have been calculated because for ^{18}F-FDG PET/CT in avascular necrosis because it is a constant.

presents one of the cases with cervical medullary compression in which both WB-MR and ^{18}F-FDG PET/CT correctly detected the plasmacytoma at C7 level, although MR was more precise in evaluating cervical medullary compression.

Clinical Versus Radiological Assessment of the Response to Treatment

The analysis of the response to treatment versus clinical response is shown in Table 6 and Table 7. In the evaluation of response to treatment, we observed a good concordance between clinical and radiological response ($\kappa = 0.76$ for WB-MR and 0.63 for ^{18}F-FDG PET/CT; $P < 0.0001$ for both).

In our study, the WB-MR had 2 false positives, one related to a chronic osteomyelitis of the pelvis and the other related to a case of osteonecrosis, in both cases with negative ^{18}F-FDG PET/CT results in those locations. On the other hand, ^{18}F-FDG PET/CT presented 2 false positives, one due to acute rib fractures and the other due to an osteonecrosis of the mandible secondary to a treatment with bisphosphonates.

DISCUSSION

In this study, we retrospectively compared WB-MR and ^{18}F-FDG PET/CT in the initial staging and response assessment at the end of treatment in MM. In 2014, the updated diagnosis criteria for MM included ^{18}F-FDG PET/CT and MR.[3] However, there are limited studies addressing the specific role of MR and ^{18}F-FDG PET/CT in the management algorithm of MM.

Our results in the study of the skull show lytic lesions in 16 cases in SS; one of these cases was not detected with WB-MR, and 3 of them with ^{18}F-FDG PET/CT. These findings are in agreement with other studies and suggest that this is the only location where SS remains useful. In this region, agreement coefficient between WB-MR and ^{18}F-FDG PET/CT is good ($\kappa = 0.819$; $P < 0.0001$), whereas agreement between these techniques and SS evidences limitations in both for WB-MR ($\kappa = 0.59$; $P < 0.002$) and for ^{18}F-FDG PET/CT ($\kappa = 0.48$; $P < 0.02$). Whole-body MR shows lower resolution and image quality than the skull-focused MR studies. In ^{18}F-FDG PET/CT, high brain ^{18}F-FDG metabolism limits the analysis of the metabolism in the skull.[1,11]

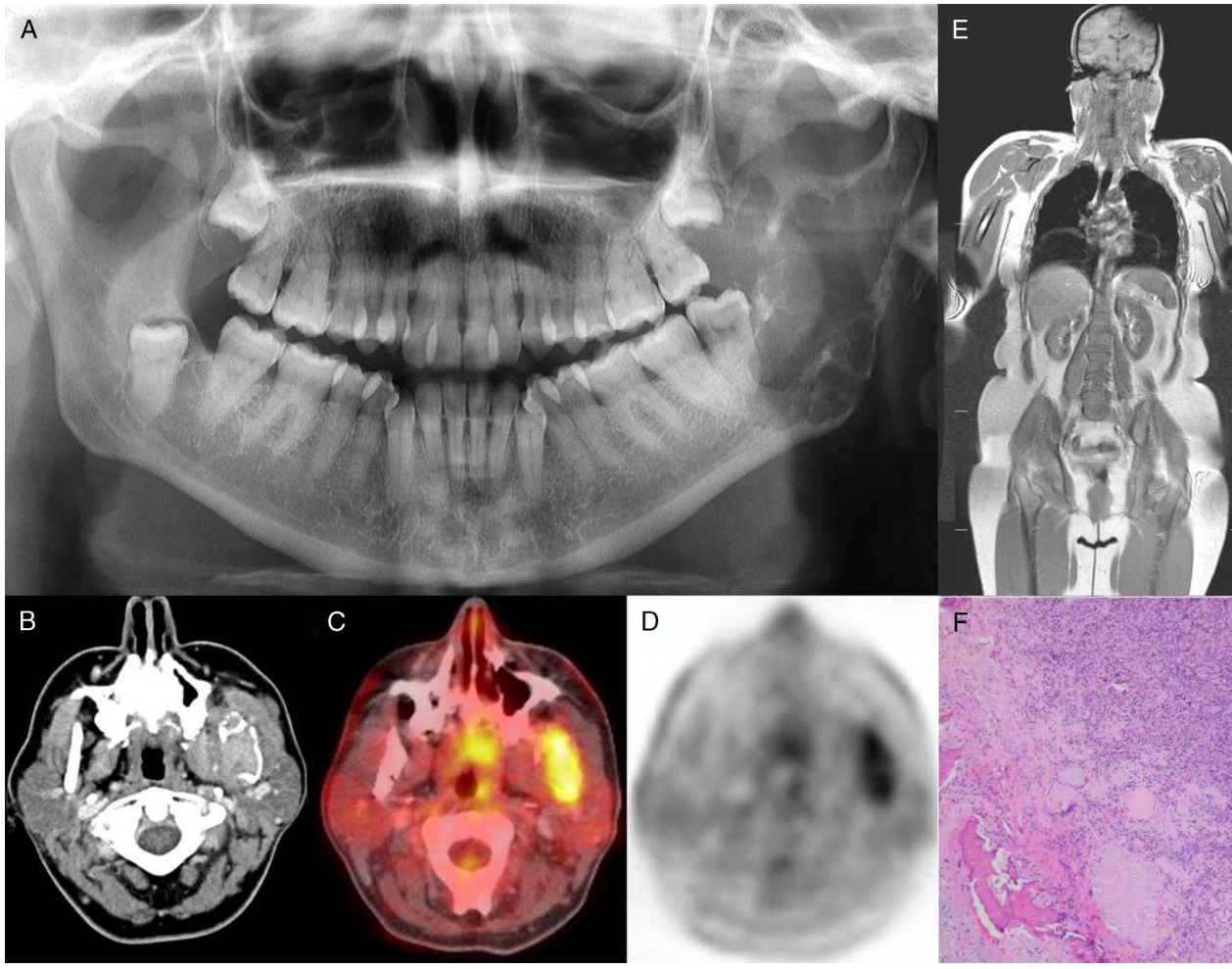

FIGURE 4. This 46-year-old woman presented with an expansive lytic lesion at the mandibular angle and in the left ascending limb, as shown in the orthopantomography (**A**). The tumor destroys the cortical bone and infiltrates the masticatory space with an associated soft tissue mass, visible on CT (**B**). ^{18}F-FDG PET/CT shows intense ^{18}F-FDG uptake (SUVmax 7.4) in the lesion, as shown in the axial fused ^{18}F-FDG PET/CT fusion (**C**) and axial ^{18}F-FDG PET (**D**). Whole-body MR only shows the mandibular lesion (**E**). Biopsy of the lesion showed diffuse proliferation of plasma cells compatible with plasmacytoma (**F**). Immunohistochemistry demonstrated monoclonal lambda light chains in her plasma cells.

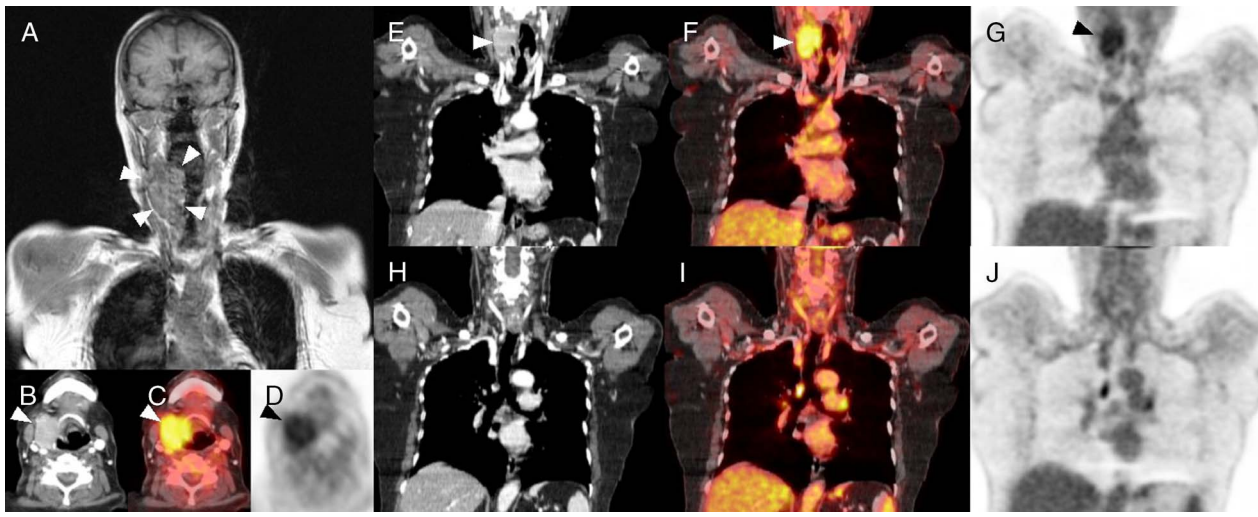

FIGURE 5. A 72-year-old woman diagnosed with MM who achieved a complete remission following an autologous peripheral blood stem cell transplant 10 years before. The patient was studied because of suspected relapse. Imaging confirmed a nodal recurrence in the neck and mediastinum, as seen in the WB-MR (**A**) and in the ^{18}F-FDG PET/CT. Here we present ^{18}F-FDG PET/CT images showing the high ^{18}F-FDG uptake in the right cervical conglomerate lymphadenopathy as can be seen in the axial CT (**B**), fused ^{18}F-FDG PET/CT (**C**), and ^{18}F-FDG PET (**D**), as well as in the coronal CT (**E**), fused ^{18}F-FDG PET/CT (**F**), and ^{18}F-FDG PET (**G**). The patient was treated with local radiotherapy and corticoid therapy (dexamethasone), achieving a complete remission evidenced by the absence of metabolic tumor activity in the ^{18}F-FDG PET/CT study, as can be seen in the following coronal images of CT (**H**), fused ^{18}F-FDG PET/CT (**I**), and ^{18}F-FDG PET (**J**). Whole-body MR was not done in the follow-up.

We observed very good agreement between WB-MR and ^{18}F-FDG PET/CT in lesions in the dorsal and lumbar column ($\kappa = 0.83$ and 0.79, respectively; $P < 0.0001$ for both). We found lower agreement in the cervical spine in WB-MR versus ^{18}F-FDG PET/CT ($\kappa = 0.59$; $P < 0.0001$), whereas SS detected very few lesions in all these locations. These findings have been described in previous studies.[6]

The study of the sternum and ribs showed a good agreement between WB-MR and ^{18}F-FDG PET/CT ($\kappa = 0.65$ and 0.72, respectively; $P < 0.0001$ for both). On the other hand, SS did not detect any

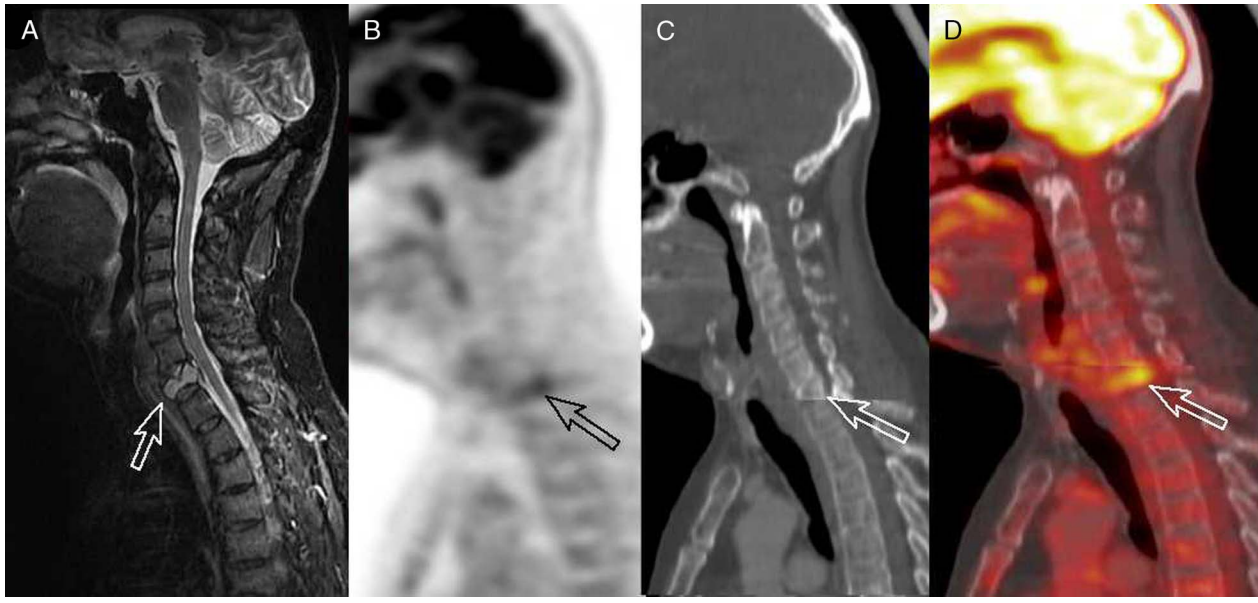

FIGURE 6. This 55-year-old man with MM achieved a complete remission following an autologous stem cell transplant 1 year before. He was studied because of suspected relapse, presenting neck pain. Imaging confirmed a plasmacytoma at C7 level with epidural and prevertebral soft tissue mass and cervical medullary compression, as shown in the STIR sequences of the cervical spine (**A**). ^{18}F-FDG PET/CT was positive, showing high ^{18}F-FDG uptake with SUVmax 6.7, as can be seen in the sagittal ^{18}F-FDG PET/CT images presented here, corresponding to the ^{18}F-FDG PET (**B**), the CT component of the PET/CT (**C**), and the fused ^{18}F-FDG PET/CT image (**D**). Following further treatment with radiotherapy and chemotherapy, the patient reached a complete remission, remaining in this situation after 2 years of follow-up.

TABLE 7. Agreement or Concordance Between Posttreatment (or Response Assessment) Clinical and Radiological Information Regarding the Patients Studied

Agreement Between Radiological and Clinical Response Assessment for Patients

		Clinical			Agreement	
Radiological		**CRs, CR, VGPR**	**PR, SD**	**PD**	**κ**	***P***
MR						
MR	CR	16	0	0	0.763	0.0001
	PR/SD	3	3	0		
	PD	1	0	7		
PET/CT						
PET/CT	CR	15	0	0	0.631	0.0001
	PR/SD	3	2	0		
	PD	2	1	6		

CRs, strict complete response; CR, complete response; PD, progressive disease; PR, partial response, SD, stable disease; VGPR, very good partial response.

lesions in the sternum, which is a great limitation to this technique. When it comes to evaluating rib involvement, only the largest lytic lesions were detected with SS. Our findings are in accordance with previous studies.[6,14]

In the pelvis, the concordance between WB-MR and ^{18}F-FDG PET/CT was good ($\kappa = 0.74$; $P < 0.0001$), whereas SS had the same limitations as in the sternum and ribs.[6,11,14]

In the upper and lower limbs, the concordance between WB-MR and ^{18}F-FDG PET/CT was excellent ($\kappa = 0.93$ and 0.83, respectively, $P < 0.0001$ for both) and good in the clavicles ($\kappa = 0.78$; $P < 0.0001$), whereas in the same regions, the concordance of both techniques with the SS was minimal.

Multiple myeloma can present with lymphadenopathy at the onset or during disease progression or relapse, the same as in other hematological malignancies.[15] In our study, ^{18}F-FDG PET/CT has shown a better performance than WB-MR in this location.

Plasmacytomas in the bone are frequent in the context of MM. Extralymphatic plasmacytomas can appear in any location, and a pathological study is necessary for diagnosis.[16] In our study, the evaluation of plasmacytomas showed a good correlation between WB-MR and ^{18}F-FDG PET/CT ($\kappa = 0.84$; $P < 0.0001$).

In the evaluation of the response to treatment, we observed a good concordance between clinical and radiological response ($\kappa = 0.76$ for WB-MR and 0.63 for ^{18}F-FDG PET/CT; $P < 0.0001$ for both). As described in the literature, WB-MR seems to provide better results than ^{18}F-FDG PET/CT at diagnosis and in relapse. However, in the evaluation of the response to treatment, WB-MR may give false positives due to residual lesions without tumor activity, and therefore ^{18}F-FDG PET/CT may be more adequate to assess the complete remission/response status.[8,9,17–20] In our series, we had 2 cases in which WB-MR was positive in the pelvis, but ^{18}F-FDG PET/CT was negative, corresponding to a chronic osteomyelitis in one case and an osteonecrosis in the other. We also had 2 false positives for ^{18}F-FDG PET/CT. One patient had acute rib fractures with ^{18}F-FDG uptake. In the other, there was intense ^{18}F-FDG uptake in the lower jaw corresponding to an osteonecrosis secondary to treatment with bisphosphonates. In both cases, WB-MR was negative, and the patients were clinically in complete remission.

Recent studies incorporate very promising new radiopharmaceuticals such as ^{11}C-methionine, with a diagnostic superiority over ^{18}F-FDG in MM, with a good correlation between radiotracer uptake and bone marrow involvement,[21] as ^{18}F-FDG evaluates glucose consumption, whereas ^{11}C-methionine depicts protein synthesis. Other tracers are being evaluated in monitoring response to treatment in MM,[19,20] although there is still no consensus on their utilization.[4,22] Furthermore, a clinical trial compared 2 branches, one with WB-MR and the other with ^{18}F-FDG PET/CT in 134 patients at initial diagnosis, at interim treatment, monitoring response to therapy, and evaluating the prognosis. It found no differences between both branches.[22]

Given the success of WB-MR and ^{18}F-FDG PET/CT, PET/MR appears to have a very promising future for the evaluation of MM, although the current available data are very limited.[20,23]

Strengths of the Study

The main strength of this study is the analysis of both tests, WB-MR and ^{18}F-FDG PET/CT, at initial diagnosis and follow-up. The only previous study comparing both tests at the same time point with a maximum time frame (or range) of 30 days between both tests has just been published.[22]

Limitations of the Study

This study is not free of limitations: (*a*) the limitations of the patient population include problems in the inclusion of patients because of the fact that it was a retrospective study and (*b*) the limitations of the evaluation of the clinical images such as the possibility of underestimation or overestimation.

CONCLUSIONS

The integral study of MM must include WB-MR and/or ^{18}F-FDG PET/CT. Skeletal survey has many limitations to evaluate MM lesions except for those in skull. Whole-body MR and ^{18}F-FDG PET/CT are complementary techniques, because both of them show good concordance in almost every location. We can evaluate spinal column with both WB-MR and ^{18}F-FDG PET/CT. However, given the better detection of lesions in the cervical spine and complications such as medullar compression, WB-MR may be the best diagnostic technique. It is necessary to individualize their use according to patient characteristics.

REFERENCES

1. Fonti R, Salvatore B, Quarantelli M, et al. ^{18}F-FDG PET/CT, ^{99m}Tc-MIBI, and MRI in evaluation of patients with multiple myeloma. *J Nucl Med*. 2008;49:195–200.
2. Walker RC, Brown TL, Jones-Jackson LB, et al. Imaging of multiple myeloma and related plasma cell dyscrasias. *J Nucl Med*. 2012;53:1091–1101.
3. Rajkumar SV, Dimopoulos MA, Palumbo A, et al. International myeloma working group updated criteria for the diagnosis of multiple myeloma. *Lancet Oncol*. 2014;15:e538–e548.
4. Rubini G, Niccoli-Asabella A, Ferrari C, et al. Myeloma bone and extra-medullary disease: role of PET/CT and other whole-body imaging techniques. *Crit Rev Oncol Hematol*. 2016;101:169–183.
5. Rajkumar V. Myeloma today: disease definitions and treatment advances. *Am J Hematol*. 2016;91:90–100.
6. Hanrahan CJ, Christensen CR, Crim JR. Current concepts in the evaluation of multiple myeloma with MR imaging and FDG PET/CT. *Radiographics*. 2010;30:127–142.
7. Dimopoulos M, Terpos E, Comenzo RL, et al. International Myeloma Working Group consensus statement and guidelines regarding the current role of imaging techniques in the diagnosis and monitoring of multiple myeloma. *Leukemia*. 2009;23:1545–1556.
8. Regelink JC, Minnema MC, Terpos E, et al. Comparison of modern and conventional imaging techniques in establishing multiple myeloma-related bone disease: a systematic review. *Br J Haematol*. 2013;162:50–61.
9. Bartel TB, Haessler J, Brown TL, et al. F18-fluorodeoxyglucose positron emission tomography in the context of other imaging techniques and prognostic factors in multiple myeloma. *Blood*. 2009;114:2068–2076.
10. Zamagni E, Patriarca F, Nanni C, et al. Prognostic relevance of 18-F FDG PET/CT in newly diagnosed multiple myeloma patients treated with up-front autologous transplantation. *Blood*. 2011;118:5989–5995.

11. Ferraro R, Agarwal A, Martin-Macintosh EL, et al. MR imaging and PET/CT in diagnosis and management of multiple myeloma. *Radiographics*. 2015;35:438–454.
12. Jadvar H, Colletti PM, Delgado-Bolton R, et al. Appropriate use criteria for ^{18}F-FDG PET/CT in restaging and treatment response assessment of malignant disease. *J Nucl Med*. 2017;58:2026–2037.
13. Boellaard R, Delgado-Bolton R, Oyen WJ, et al. FDG PET/CT: EANM procedure guidelines for tumour imaging: version 2.0. *Eur J Nucl Med Mol Imaging*. 2015;42:328–354.
14. Lecouvet FE. Whole-body MR imaging: musculoskeletal applications. *Radiology*. 2016;279:345–365.
15. Dayton VD, Williams SJ, McKenna RW, et al. Unusual extramedullary hematopoietic neoplasms in lymph nodes. *Hum Pathol*. 2017;62:13–22.
16. Jeyaraj P, Venkatesan M, Nijhawan VS. Solitary extramedullary plasmacytoma of the maxillary sinus, progressing to smoldering multiple myeloma with multifocal skeletal involvement, which resolved completely following chemotherapy alone. *J Maxillofac Oral Surg*. 2016;15(suppl 2):229–239.
17. Terpos E, Kleber M, Engelhardt M, et al. European myeloma network guidelines for the management of multiple myeloma-related complications. *Haematologica*. 2015;100:1254–1266.
18. Derlin T, Peldschus K, Münster S, et al. Comparative diagnostic performance of ^{18}F-FDG PET/CT versus whole-body MRI for determination of remission status in multiple myeloma after stem cell transplantation. *Eur Radiol*. 2013;23:570–578.
19. de Waal EGM, Glaudemans AWJM, Schröder CP, et al. Nuclear medicine imaging of multiple myeloma, particularly in the relapsed setting. *Eur J Nucl Med Mol Imaging*. 2017;44:332–341.
20. Nanni C, Zamagni E. Therapy assessment in multiple myeloma with PET. *Eur J Nucl Med Mol Imaging*. 2017;44(Suppl. 1):111–117.
21. Lapa C, Knop S, Schreder M, et al. ^{11}C-methionine-PET in multiple myeloma: correlation with clinical parameters and bone marrow involvement. *Theranostics*. 2016;6:254–261.
22. Moreau P, Attal M, Caillot D, et al. Prospective evaluation of magnetic resonance imaging and ^{18}F-fluorodeoxyglucose positron emission tomography–computed tomography at diagnosis and before maintenance therapy in symptomatic patients with multiple myeloma included in the IFM/DFCI 2009 trial: results of the IMAJEM study. *J Clin Oncol*. 2017;35:2911–2918.
23. Shah SN, Oldan JD. PET/MR imaging of multiple myeloma. *Magn Reson Imaging Clin N Am*. 2017;25:351–365.